



Quark and Lepton Masses from Renormalization Group Fixed Points

CHRISTOPHER T. HILL

Fermi National Accelerator Laboratory, Batavia, Illinois 60510

(Received

ABSTRACT

The renormalization group equations describing the evolution of fermion Higgs-Yukawa coupling constants down from M_x in a Grand Unified Theory possess fixed points which may lead to universal predictions for fermion masses independent of symmetry considerations at M_x . Our analysis predicts ≈ 240 GeV for the fixed point t-quark mass. Alternatively, a sufficiently heavy fourth SU(5) generation cannot be ruled out by existing bounds on n_f and we find fixed point mass predictions of $m_T \approx 219$ GeV, $m_B \approx 215$ GeV and $m_E \approx 60$ GeV.

PACS Category Nos.: 12.20.Hx, 14.80.Dq



I. INTRODUCTION

One of the great problems of particle physics is to understand the origin and to calculate the values of the elementary fermion, i.e. quark and lepton, masses observed in the laboratory. There have been many proposals for dealing with this question involving, typically, the imposition of some kind of discrete symmetry or, perhaps equivalently, to view it as a consequence of constraints arising in grand unified theories at very short distances.¹ Indeed, one of the triumphs of SU(5) is the successful prediction of m_b/m_τ in the "minimally Higgsified" scheme. Here the short distance relationship $m_b = m_\tau$ is renormalized by evolving the Higgs-Yukawa coupling constants g_b and g_τ down from M_X ($\approx 10^{15}$ GeV) to the light fermion mass scales (\approx few GeV) where the principle effect is the increase in m_b due to QCD-gluonic radiative corrections.² As strong a vote of confidence for SU(5) as this result may be, we do not know what sets the scale of m_b ($= m_\tau$), or equivalently g_b ($= g_\tau$), at M_X . Hence, a completely satisfactory theory of fermion masses and the related problem of mixing angles is certainly lacking at present.

A novel idea has recently occurred to Pendleton and Ross which is not unrelated to the m_b/m_τ relation in SU(5). In an interesting letter³ they have suggested that the top quark, or possibly other heavy quarks, may have masses determined solely by the low energy structure of the renormalization group equations describing the evolution down from M_X to m_t ($\approx M_W$, the "terrestrial" mass scale of $SU(2) \times U(1)$ electroweak symmetry breaking). Here the top quark mass is determined by an infra-red stable "quasi"-fixed point of the RG equations and one, in principle, obtains a universal result for the physical m_{top} over a large range of initial g_{top} Higgs-Yukawa couplings at M_X . We refer to this behavior as a "quasi"-fixed point because, as Pendleton and Ross show, g_t is swept toward a value of $\sqrt{2/9} g_{\text{QCD}}(\mu^2)$ and continues to track the strong coupling constant for

sufficiently small final mass scales, μ^2 . Hence, Pendleton and Ross predict upon including additional $SU(2) \times U(1)$ corrections that the top quark will weigh in at about 135 GeV, if it is already in the domain of this fixed point behavior at that energy scale.

This possibility is quite intriguing because it illustrates that the details of the precise symmetry conditions determining particle masses (or their Higgs-Yukawa couplings) at a primordial mass scale can be completely obliterated by the renormalization group and replaced by the fixed point structure of the RG equations themselves. Furthermore, if such a mechanism is operant, we may in principle already possess an understanding of the relevant RG equations but have no inkling as to the underlying symmetry conditions at $M_{\text{primordial}}$, having nonetheless a prediction for the fermion masses. We shall see, furthermore, that the effect that increases m_b relative to m_τ in $SU(5)$ is precisely the strong interaction renormalization which principally gives the Pendleton-Ross fixed point behavior for g_{top} . Hence, the successful m_b/m_τ relationship may also be a strong vote of confidence for the existence of a real fixed point behavior for a much heavier fermion such as the top quark.

The Pendleton-Ross fixed point represents the exact mathematical fixed point structure of the renormalization group equations for g_{top} and g_{QCD} . This is an attractive fixed point in the sense that as one proceeds toward decreasing μ^2 , one should be pulled toward the fixed point for arbitrary initial $g_{\text{top}}(M_x)$. In fact, one finds that this fixed point is never significantly approached for final μ^2 as large as $\approx M_W^2$ and is not reached until $\mu^2 \ll 1 \text{ GeV}^2$ whence g_{QCD}^2 begins to vary dramatically. The authors of ref. (3) note that numerically their exact fixed point corresponds to $\sim 135 \text{ GeV}$ for m_{top} (including electroweak corrections) whereas the solution to the renormalization group equations actually allows m_{top} in the range of 110 to 220 GeV.

Nevertheless, we show that there is yet another "intermediate fixed point" behavior of the solution to the RG equations that is relevant at $\mu^2 \approx m_t^2$. Whereas the Pendleton-Ross fixed point behavior is obtained by studying simultaneously the RG equations for g_t^2 and g_{QCD}^2 , our result is obtained by treating g_{QCD}^2 as "slowly varying" and replacing it by a constant, \bar{g}_{QCD}^2 , in the RG equations for g_t^2 by itself. To a good approximation \bar{g}_{QCD}^2 is just the average of $g_{\text{QCD}}^2(\mu)$ over the range $m_t^2 \leq \mu^2 \leq M_x^2$ (though we give an optimization of \bar{g} valid also in the cases studied in Section III involving multiple heavy quarks). In this manner we obtain a precise prediction for m_t larger than that of ref. (3). Indeed, we obtain $m_t \approx 240$ GeV including the full electroweak corrections using the values of $\langle \phi^0 \rangle = v/\sqrt{2} = 175$ GeV of ref. (3, 10). This result is valid to one loop and we expect possible significant corrections in two loops principally from QCD. This result is also consistent with an upper bound quoted by the authors of ref. (3) of $m_t \approx 220$ GeV keeping only QCD effects in discussing the rate of approach to their fixed point. We will show however that this mass value is the actual relevant fixed point obtained from the RG equation for g_t at these mass scales. The prediction emerges from the simple assumption of an $SU(2) \times U(1) \times SU(3)$ desert beyond the top quark for $m_t \leq \mu \leq M_x$.

To illustrate the existence of the intermediate fixed point behavior the result for g_t (100 GeV) is plotted against g_t ($M_x \sim 10^{15}$ GeV) in Fig. (1), keeping only QCD effects (m_t is given by $m_t \approx g_t(100 \text{ GeV}) \times v/\sqrt{2}$). The intermediate fixed point is the asymptotically constant behavior of this curve at $g_t(100) \approx 1.27$ whereas the Pendleton-Ross fixed point is indicated by the dashed line. The PR fixed point is clearly not controlling the actual asymptotic behavior. Also, we note presently that the asymptotic value of this function provides an absolute upper bound for the mass of any $+2/3$ charged quark to one loop order, keeping only the effects of QCD. We improve the result quantitatively in Section II. We also indicate in Fig. (1) a crude estimate of the intermediate fixed point behavior by using for \bar{g}_{QCD}^2 the

average of g_{QCD}^2 with respect to $t = \ln \mu$ over the range $100 \leq \mu \leq 10^{15}$ GeV. This result is seen to be much closer and, in fact, we show in Section II how to compute the exact asymptote from the intermediate fixed point analysis.

Such large masses for the t-quark may seem to be unrealistic;²² it may well be that $g_t(M_X)$ is not initially large enough to be swept toward the intermediate fixed point, even though it is likely to suffer a large upward renormalization through the effects of QCD in evolving down from M_X . In that case our discussion of single heavy fermion RG fixed points is irrelevant, but the possibility remains that there exists a fourth generation of heavy quarks and leptons for which RG fixed point behavior becomes extremely likely. Indeed, the usual bound on n_f may accommodate at least one more,⁴ whereas the strict limit $n_f \leq 6$ of Nanopoulos and Ross,⁵ in examining two loop effects, may become invalid if there are heavy quarks and leptons whose Higgs-Yukawa couplings are comparable to g_{QCD} . Therefore, in Section III we analyze the case of a single heavy quark pair and a complete SU(5) heavy fermion generation with arbitrary g_U and $g_D = g_E$ at M_X . We make the simplifying assumption of no Cabibbo mixing with the other generations and ignore heavy neutrino contributions. We obtain scatter plots which represent the probability of finding fermions in given mass ranges assuming only the existence of the desert. Most of our points are seen to cluster about an intermediate fixed point and, in the case of a single heavy SU(5) generation, we obtain the most probable values for the masses:

$$m_U \approx 219 \text{ GeV} \quad m_D \approx 215 \text{ GeV} \quad m_E \approx 60 \text{ GeV} \quad .$$

Again, we find that the fixed point behavior of physical interest is roughly determined by the average values of the QCD and electroweak coupling constants over the region of integration.

Finally, in Section IV we review various constraints and examine other consequences of our mechanism. For example, to what extent is the m_b/m_τ relationship affected by the existence of heavy fermions which have Higgs-Yukawa couplings of order g_{QCD} ? Our essential conclusion is consistent with that of Pendleton and Ross, even in the case of many heavy fermions, that one cannot rule this possibility out. Hence, one might reasonably expect to find massive quarks in the $m_q \approx 200$ to 250 GeV range and leptons in the neighborhood of ≈ 60 GeV.

We mention that these discussions are related to earlier works placing bounds upon the numbers and masses of quarks and leptons as in Maiani et al.⁶ We believe that the fixed points are more than mere bounds as they are the most probable places that the masses will accumulate at μ^2 given an approximately flat probability distribution at M_x^2 . Also, there has been an effort to understand the hierarchies of mixing angles and fermion masses in terms of the renormalization group a la Frogatt and Nielson.⁷ The conclusions of ref. (7) are essentially realized in ref. (3) and the present work in that, in the absence of discrete symmetries one finds two hierarchies consisting of "light" fermions, (u,d,c,s,b), whose Higgs-Yukawa couplings are not sufficiently large to be within the domain of attraction of the non-trivial fixed point and "heavy" fermions including perhaps the t-quark and conceivably successive generations which are strongly influenced by the fixed points. As in ref. (3) and ref. (7), we have no comment on the distribution of light quark masses, which are sensitive to the primordial symmetry relationships.

Also, recently Veltman has considered the problem of quadratic divergences and the necessity of imposing cancellations of these in any realistic dynamical symmetry breaking, i.e. composite Higgs boson, schemes.⁸ These considerations lead to similar heavy mass predictions and may be related to the present work and ref. (3) in which fixed points essentially imply the cancellation of logarithmic

divergences. Finally, Ross and Pendleton are extending their analysis to other problems.⁹

Presently we shall consider the case of a single heavy t-quark neglecting Higgs-Yukawa corrections of known fermions and various corrections beyond one-loop.

II. CASE FOR A HEAVY TOP QUARK

We assume presently that there are no heavy fermions beyond the t-quark, with the possible exception of super-heavies which have masses of order M_X and have thus decoupled for momentum scales $\mu \ll M_X$. The Yukawa coupling constant of the top quark to a single doublet of Higgs bosons determines the mass of the top quark through the equation (we follow the conventions of Sakurai¹⁰):

$$m_t = \frac{v}{\sqrt{2}} g_t \left(-\lambda m_t^2, -\lambda m_t^2, 0 \right) \quad (2.1)$$

where g_t is evaluated at zero momentum transfer to the Higgs boson and $v/\sqrt{2}$ is the Higgs vacuum expectation value. v is determined by the W-boson mass and the SU(2) coupling constant g :

$$M_q = gv/\sqrt{2} \quad ; \quad v \approx 245 \text{ GeV} \quad (2.2)$$

with $M_w \approx 78 \text{ GeV}$, and $\sin^2 \theta_w \approx .23$. λ in eq. (2.1) is a "threshold factor" of order unity.

The running Higgs-Yukawa coupling constant, $g(-\mu^2) \equiv g(-\mu^2, -\mu^2, -\mu^2)$, satisfies the renormalization group equation to order one loop¹¹:

$$16\pi^2 \frac{dg_t}{dt} = g_t \left\{ \frac{9}{2} g_t^2 - 8g_c^2 - \kappa_t(t) \right\} \quad (2.3)$$

where $t = \ln \mu$ and we've neglected the contributions of the lighter quarks and leptons, and

$$\kappa_t(t) = \frac{9}{4} g^2(t) + \frac{17}{12} g'^2(t) \quad (2.4)$$

Here g_c , g and g' are, respectively, the coupling constants of SU(3), SU(2), and U(1).

The running of g_t described by eq. (2.3) is appropriate to the coupling constant evaluated at a symmetrical point in momentum space and we must consider the extrapolation from the case of zero momentum transfer in eq. (2.1) which determines the fermion mass.¹² This is analogous to the extrapolation of α_{EM} from the Thomson limit of Compton scattering ($=1/137$) to $-q^2 = \lambda M_w^2$ ($\approx 1/128$). The extrapolation involves the diagrams of Fig. (2b), which are of order $\kappa_t g_t$, and those of Fig. (2c) which are of order $g_t g_\ell^2$ with g_ℓ a light fermion Yukawa coupling. The latter contributions are by themselves gauge invariant, but we are tacitly ignoring terms of order g_ℓ^2 in eq. (2.3) and will thus ignore these. The corrections of order $\kappa_t g_t$ are in principle a problem and constitute a gauge dependence in the Higgs vacuum polarization and in the extrapolation. However, we expect these effects to contribute only in the range $\lambda M_w^2 < \mu^2 < \lambda m_t^2$ and in practice this is not a significant contribution. Also, there are no extrapolation effects for $\mu^2 < \lambda m_t^2$ of order g_t^3 . Hence, we have to a very good approximation:

$$g_t(-\mu^2, -\mu^2, 0) \approx g_t(-\mu^2, -\mu^2, -\mu^2) \Big|_{\mu^2 \leq \lambda m_t^2} . \quad (2.5)$$

The running of g_t described by eq. (2.3) will terminate by decoupling for $\mu^2 \leq \lambda m_t^2 = \lambda g_t^2 v^2/2$, and the quantity of interest to us is therefore:

$$m_t = \frac{v}{\sqrt{2}} g_t \left(-\lambda m_t^2, g_t(M_x^2) \right) . \quad (2.6)$$

For our present discussion we will simply replace λm_t^2 by $\approx (100)^2 \text{ GeV}^2$ in evaluating m_t and later we will consider the solution of this implicit equation by Newton's method, which leads to a correction of order a few percent. λ is here associated principally with the $t \rightarrow t + \text{gluon}$ threshold and is approximately unity. Henceforth we assume $\lambda = 1$.

Pendleton and Ross discovered a "quasi"-fixed point behavior by combining eq. (2.3) with the RG equation satisfied by the QCD strong-interaction coupling constant:

$$16\pi^2 \frac{dg_c}{dt} = -b_0 g_c^3 ; \quad b_0 = 11 - \frac{2}{3} n_f . \quad (2.7)$$

Upon forming the difference between eq. (2.3) and eq. (2.7) and presently ignoring κ_t , one obtains:

$$16\pi^2 \frac{d}{dt} \{ \ln(g_t/g_c) \} = \frac{9}{2} g_t^2 - (8 - b_0) g_c^2 . \quad (2.8)$$

Therefore, if the rhs of eq. (2.8) vanishes, then g_t and g_c are in a fixed ratio which remains constant for all subsequent t . Furthermore, as t tends toward zero (we will generally consider t to be decreasing from $\ln M_x$ to $\ln m_t$) any arbitrary g_t is attracted toward this fixed ratio:

$$g_t^2 = \frac{2}{9} (8 - b_0) g_c^2 \quad (2.9)$$

and subsequently g_t "tracks" along with g_c for decreasing t (we study the stability of fixed points in Section III). If such a behavior has set in for $t \approx \ln m_t$, then we will have an unambiguous prediction for m_t by eq. (2.9). For 6 quarks, $b_0 = 7$ and taking a value of $\alpha_s = g_c^2/4\pi \approx 1/7$ at $100 \text{ GeV} = \mu$ yields $m_t \approx 110 \text{ TeV}$ which is the Pendleton-Ross prediction for m_t in the absence of electroweak (κ_t) corrections (these increase m_t to $\approx 135 \text{ GeV}$).

The exact solution of eq. (2.3), neglecting κ_t , is:

$$g_t^2(\mu^2) = g_t^2(M_x^2) \left(\frac{g_c^2(\mu^2)}{g_c^2(M_x^2)} \right)^{8/b_0} \left\{ 1 + \frac{9g_t^2(M_x^2)}{2g_c^2(M_x^2)} \left(\left(\frac{g_c^2(\mu^2)}{g_c^2(M_x^2)} \right)^{1/b_0} - 1 \right) \right\}^{-1} \quad (2.1)$$

One sees in eq. (2.10) that in the limit:

$$\left(\frac{g_c^2(\mu^2)}{g_c^2(M^2)} \right)^{1/b_0} \gg 1 \quad (2.11)$$

we reach the PR fixed point behavior:

$$g_t^2(\mu^2) = \frac{2}{9} \left(\frac{g_c^2(\mu^2)}{g_c^2(M_x^2)} \right)^{7/b_0} g_c^2(M_x^2) \quad (2.12)$$

which is a fixed point in the sense that all information about the boundary condition, $g_t(M_x^2)$, has dropped out. Remarkably, the case $n_f = 6$ is quite special since with $b_0 = 7$ all information about M_x^2 also drops out, and we obtain

$$g_t^2(\mu^2) = \frac{2}{9} g_c^2(\mu^2) \quad (2.13)$$

Note that eq. (2.12) is also equivalent to eq. (2.9) plus small logarithmic corrections.

Our principle concern, however, is whether one is justified in assuming that the PR fixed point behavior has set in by the time one reaches mass scales of order λm_t in evolving down from $t = \ln M_x$. Of course, we have the exact solution of eq. (2.3) in eq. (2.10), but in the more complicated case of several heavy fermions as discussed in Section III this will not be available to us and an understanding of the relevant mechanisms becomes essential. In fact a closer examination of the solution eq. (2.10) reveals that the PR fixed point does not set in until $\mu < 1$ GeV.

First, let us examine the solution's properties graphically. In Fig. (3) we've plotted the exact solution of eq. (2.10) for $g_t(\mu^2)$ as a function of $g_t(M_x^2)$ for three sample values of μ^2 . The details of our choice of a specific $g_c^2(t)$ may be found toward the latter part of this section. We've also indicated the point on each curve at which eq. (2.13) is satisfied. We see that the approach to the PR fixed point is quite slow and does not seem to be reflected in the location of the constant asymptote until $\mu < 1$ GeV. Nevertheless, the curves possess a constant asymptotic behavior as $g_t(M_x^2)$ gets large for each choice of μ^2 (of course, we require that

$(g_t^2(M_x^2))/(16\pi^2) \ll 1$ lest eq. (2.3) be disfigured by higher order corrections). This asymptotic constant behavior literally implies the existence of some kind of fixed point behavior since $g_t(\mu^2)$ is independent of $g_t(M_x^2)$ as the latter becomes sufficiently large. What accounts for this behavior which is evidently independent of the Pendleton-Ross fixed points?

First we will give a schematic description. Consider eq. (2.3) by itself without forming the combined equation (2.8). Over the domain of integration where μ varies from between $\approx 10^{15}$ to $\approx 10^2$ we may consider the behavior of g_t to be "relatively constant," varying from $\approx 1/50$ to $\approx 1/7$. If we begin with $g_t(10^{15})$ sufficiently large, much of the initial evolution of $g_t(\mu)$ is given solely by the first term on the rhs of eq. (2.3). Indeed, if $9/2 g_t^2(\mu^2) \gg 8g_C^2(\mu^2)$ we may ignore the effects of QCD altogether and write:

$$16\pi^2 \frac{d \ln g_t}{dt} = \frac{9}{2} g_t^2 \quad M'^2 \lesssim \mu^2 \lesssim M_x^2 \quad . \quad (2.14)$$

As μ decreases from the intermediate mass scale M' , g_t will decrease by eq. (2.14) until it "feels" the effects of the second term on the rhs of (2.3) at some scale for which $g_C(\mu) > g_C(M_x)$. Here the two terms will compete in a region in which $9/2 g_t^2 \approx 8g_C^2$, and we thus have:

$$16\pi^2 \frac{d \ln g_t}{dt} = \frac{9}{2} g_t^2 - 8g_C^2 \approx 0 \quad M''^2 \lesssim \mu^2 \lesssim M'^2 \quad . \quad (2.15)$$

In this intermediate region g_t must remain relatively constant. Finally, the rapidly increasing g_C^2 overtakes the leading term on the rhs and we eventually reach the "tracking" behavior of the PR fixed point in which the ratio of g_t/g_C becomes constant:

$$16\pi^2 \frac{d \ln(g_t/g_C)}{dt} = \frac{9}{2} g_t^2 - (8 - b_o) g_C^2 \approx 0 \quad , \quad \mu^2 \ll M'^2 \quad . \quad (2.16)$$

In fact, it is precisely the condition of eq. (2.15) which gives rise to the asymptotic behavior of the curves in Fig. (3)

$$\frac{9}{2} g_t^2 \approx 8 \bar{g}_C^2 \quad M'^2 \lesssim \mu^2 \lesssim M^2 \quad (2.17)$$

where \bar{g}_C^2 is a typical value of $g_C^2(\mu^2)$ in the intermediate range. As a preliminary estimate for the appropriate value of \bar{g}_C^2 in eq. (2.17) let us simply take the average of $g_C^2(t)$ over the range $t_o = \ln \mu$ to $t_f = \ln 10^{15}$. In fact, we a priori expect this to slightly underestimate the correct \bar{g}_C^2 since we are making no provision to cut off our averaging at $\ln M'$ and we include a tail from $\ln M'$ to $\ln M_x$ in which $g_C^2(t)$ is at its smallest values. Taking $\mu = 10^2$ for example, we find $\bar{g}_C^2 \approx .66$ whence we expect the asymptote for this curve at $g_t \gtrsim 4/3 \bar{g}_C \approx 1.08$. We've plotted these points on each curve and indeed we see they are, to a good approximation, a description of the correct asymptotic behavior, including the slight underestimate as expected. Even in the case when the PR fixed point is becoming a better approximation at $\mu = 1$ GeV, our crude result is still quite good.

Hence, our graphical analysis suggests it is not the condition of eq. (2.16) which determines the fixed point behavior of the physical Higgs-Yukawa coupling at the relevant μ^2 values, but rather the condition of eq. (2.17) for the appropriate choice of \bar{g}_C^2 wrt t , which is roughly the average of g_C^2 over the entire range of integration. However, we can easily give a more rigorous meaning to \bar{g}_C^2 .

An examination of the solution eq. (2.10) reveals that the condition of eq. (2.11) is stronger than one requires to be at a fixed point. Indeed, it is sufficient that

$$\frac{9}{2} \frac{g_t^2(M_x^2)}{g_c^2(M_x^2)} \left(\left(\frac{g_c^2(\mu^2)}{g_c^2(M_x^2)} \right)^{1/b_0} - 1 \right) \gg 1 \quad (2.18)$$

which can occur before $(g_c^2(\mu^2)/g_c^2(M_x^2))^{1/b_0}$ is much larger than unity for sufficiently small $g_c^2(M_x^2)$ and large $g_t^2(M_x^2)$. Let us define $R = g_c^2(\mu^2)/g_c^2(M_x^2)$. Then we may consider $1/b_0 \ln R$ to be a small quantity and expand eq. (2.10) assuming also eq. (2.18):

$$\begin{aligned} \lim_{g_t^2(M_x^2) \rightarrow \infty} g_t^2(\mu^2) &= \frac{2}{9} g_c^2(\mu^2) \frac{\left\{ 1 + \frac{1}{b_0} \ln R + \frac{1}{2} \left(\frac{1}{b_0} \ln R \right)^2 + \dots \right\}}{\left\{ \frac{1}{b_0} \ln R \left(1 + \frac{1}{2b_0} \ln R + \frac{1}{3!} \left(\frac{1}{b_0} \ln R \right)^2 + \dots \right) \right\}} \\ &= \frac{16}{9} \left\{ \frac{b_0}{8} \frac{g_c^2(\mu^2)}{\ln R} \right\} \left\{ 1 + \frac{1}{2b_0} \ln R + \frac{7}{12b_0^2} (\ln R)^2 + \dots \right\}. \quad (2.20) \end{aligned}$$

Hence, a more rigorous definition of \bar{g}_c^2 in the integration domain of eq. (2.17) is given by

$$\bar{g}_c^2 = \frac{b_0}{8} \left(\frac{g_c^2(\mu^2)}{\ln R} \right) \quad (2.21)$$

and the actual asymptotic behavior of $g_t(\mu)$ vs. $g_t(M_x)$ is

$$g_t(\mu) = \sqrt{\frac{2b_0}{9 \ln R}} g_c(\mu) \quad R = \frac{g_c^2(\mu^2)}{g_c^2(M_x^2)}. \quad (2.22)$$

Though eq. (2.22) bears little resemblance to the average value of $g_c^2(t)$ wrt t over the domain μ^2 to M_x^2 , it is quite close to this value in practice.

In Fig. (4) we show the evolution of $g_t(\mu^2)$ against μ^2 for several initial choices of $g_t(M_x^2)$. We include also the function of eq. (2.22) and we plot the Pendleton-Ross fixed point behavior, eq. (2.13), all with $b_0 = 7$. We see that for

$g_t(M_x^2) = 1/3$, we are almost in the PR fixed ratio initially and we follow their curve quite closely. In general, the relevant behavior is illustrated by the curves with larger $g_t(M_x^2) \geq 1$. These are seen to approach the intermediate fixed point behavior near $\ln(10^2)$ reasonably well. We've also plotted the t-quark threshold condition here, i.e. when

$$t = \frac{1}{2} \ln(\lambda g_t^2 \frac{v^2}{2})$$

or

$$g_t = \frac{\sqrt{2}}{\sqrt{\lambda v}} e^t, \quad \lambda \approx 1 \quad (2.23)$$

Hence, the running behavior described by eq. (2.8) is only relevant to the right of this latter curve and the portions to the left are unphysical. We see that all curves eventually merge with the PR fixed point for very small t , but that this is to the left of our threshold conditions. We conclude that the only possible relevant fixed point behavior here is our "intermediate" fixed point as described above.

As a point of interest we note that the intermediate fixed point may be of slight mathematical interest. The value of \bar{g}_c^2 given in eq. (2.21) depends only upon its own "rate of evolution" given by b_0 and its coefficient in the differential equation (as well as its soft dependence upon M_x^2 and, of course, μ^2). Hence, for a general problem of the form

$$\frac{dy_i}{dt} = \sum_j \alpha_{ij} y_j^3 - \beta y_i x^2, \quad \frac{dx}{dt} = -\gamma x^3 \quad (2.24)$$

we will have intermediate fixed point behavior and may substitute for x in the first equation the constant

$$\bar{x} = \frac{\gamma}{\beta} \left(\frac{x(t_f)}{\ln(x(t_f)/x(t_i))} \right) \quad (2.25)$$

independent of the values of the coefficients α_{ij} . This turns out to be relevant to the cases of many quarks and leptons analyzed in Section III. Here, the same value of \bar{g}_c^2 given in eq. (2.21) (with the appropriate b_0) determines the fixed point behavior for any number of quarks.

We now turn to a more quantitative discussion including the effects of the $SU(2) \times U(1)$ electroweak interactions by the inclusion of κ_t into eq. (2.3). In the general case of an arbitrary single heavy quark or lepton we have the RG equation:

$$16\pi^2 \frac{dg_f}{dt} = g_f \left(Ag_f^2 - Bg_c^2 - Cg^2 - Dg'^2 \right) \quad (2.26)$$

the solution of which is:

$$g_f^2(t) = g_f^2(t_0) \left(\frac{g_c^2(t)}{g_c^2(t_0)} \right)^{B/b_{03}} \left(\frac{g^2(t)}{g^2(t_0)} \right)^{C/b_{02}} \left(\frac{g'^2(t)}{g'^2(t_0)} \right)^{D/b_{01}}$$

$$\div \left\{ 1 + \frac{2Ag_f^2(t_0)}{16\pi^2} \left[\int_t^{t_0} \left(\frac{g_c^2(\tau)}{g_c^2(t_0)} \right)^{B/b_{03}} \left(\frac{g^2(\tau)}{g^2(t_0)} \right)^{C/b_{02}} \left(\frac{g'^2(\tau)}{g'^2(t_0)} \right)^{D/b_{01}} d\tau \right] \right\} \quad (2.)$$

where

$$b_{03} = 11 - \frac{2}{3}n_f \quad , \quad b_{02} = \frac{22}{3} - \frac{2}{3}n_f \quad , \quad b_{01} = -\frac{2}{3}n_f$$

and

$$t_0 = \ln M_x \quad , \quad t = \ln \mu \quad . \quad (2.28)$$

In the case of the t-quark, $A = 9/2$, $B = 8$, $C = 9/4$ and $D = 17/12$. The integral appearing in eq. (2.27) must be performed numerically in general. Hence, we require the exact form of $g_c(t)$, $g(t)$ and $g'(t)$ before proceeding.

The appropriate choice of g_c^2 amounts to the correct choice of b_0 and Λ . We have the usual one loop QCD coupling constant with $b_0 = 7$ for $n_f = 6$ in the form:

$$\alpha_s = \frac{g_c^2}{4\pi} = \frac{2\pi}{7(t - \ln \Lambda)} \quad t = \ln \mu \quad . \quad (2.29)$$

The value of Λ requires brief comment.

For $n_f = 4$ and μ^2 below the b-quark threshold, we may choose a conventional value of Λ from electroproduction fits of the order $300 \text{ MeV} < \Lambda < 500 \text{ MeV}$. As we extrapolate to higher μ^2 and excite various quark flavors we must include the modifications in b_0 . One possibility is to use the Georgi-Politzer mass dependent renormalization group equations,¹³ but a simpler and quantitatively reasonable alternative is to follow the discussion of Ellis et al.¹² in which one compensates the change in b_0 at threshold by a change in Λ by demanding continuity in α_s at the threshold. Assuming $\Lambda = 500 \text{ MeV}$ when $n_f = 4$ then continuity when extrapolating through the b-quark threshold placed at $\mu = 2m_b = 10 \text{ GeV}$ gives

$$\Lambda = 385 \text{ MeV for } 4m_t^2 > \mu^2 > 4m_b^2 \quad . \quad (2.30)$$

Further, assuming a t-quark mass of order 100 GeV and extrapolating through the t-quark threshold gives

$$\Lambda = 212 \text{ MeV for } \mu^2 > 4m_t^2, \quad m_t \approx 100 \text{ GeV} \quad (2.31)$$

to one loop accuracy. This is probably a good upper bound on Λ for our purposes. We've performed a similar extrapolation starting with $\Lambda = 300 \text{ MeV}$ for $n_f = 4$ and assuming $200 \text{ GeV} \approx m_t$ which gives $\Lambda \approx 108 \text{ MeV}$ for $\mu^2 > 4m_t^2$. Hence, we have:

$$212 \text{ MeV} > \Lambda > 108 \text{ MeV} \quad \text{or} \quad -1.55 > \ln \Lambda > -2.22 \quad (2.32)$$

We will use the upper bound of 212 MeV in our subsequent analysis which will slightly overestimate m_t .

For the remaining electroweak coupling constants we simply assume $n_f = 6$, $\alpha_{EM}(M_W) \approx 1/128$ and $\sin^2 \theta_w(M_W) \approx .23$ with $M_W \approx 78 \text{ GeV}$. We are led to the following approximate one loop results:

$$\alpha_2 = \frac{g^2}{4\pi} = \frac{3\pi}{5(t + 51.05)}$$

$$\alpha_1 = \frac{g'^2}{4\pi} = \frac{3\pi}{6(159.95 - t)} \quad (2.33)$$

These are seen to unify within a few percent at $\sim 10^{15}$ to 10^{16} GeV with $\alpha_s(10^{15}) \approx 0.24$, $\alpha_2(10^{15}) \approx .022$, $\alpha_1(10^{15}) \approx .0125$ and $8/3 \sin^2 \theta_w(10^{15}) \approx .97$ (slightly better at $.5 \times 10^{17} \text{ GeV}$) all within one loop accuracy.

We can now obtain real predictions for the mass of the t-quark as follows. The mass is a function of $g_t(M_X)$ given implicitly by

$$M_t = \frac{v}{\sqrt{2}} g_t(m_t, g_t(M_X)) \quad (2.34)$$

where v is a constant ≈ 246 GeV. We apply "Newton's" method to obtain $m_t(g_t(M_X))$ iteratively by (A) choosing an initial value $m_t = m_1$, (B) substituting into rhs of eq. (2.34) and deducing a new value $m_t = \frac{v}{\sqrt{2}} g_t(m_1, g_t(M_X))$ and (C) Go to (B). The method converges very quickly in practice requiring no more than 4 iterations with $m_1 = 100$ GeV. The self-consistency condition slightly accelerates the rate of approach to the fixed point and slightly reduces the fixed point values, as expected, from those at 100 GeV. We do this comparison since in Section III we do not worry about the self-consistency constraint and expect slight overestimates of about 3% if we choose $t_f = \ln(100 \text{ GeV})$.

Our final prediction for the intermediate fixed point value of m_t including all $SU(3) \times SU(2) \times U(1)$ effects to one-loop accuracy is $m_t = 240 \text{ GeV}$. The inclusion of two-loop effects will probably increase this prediction.

Is this a reasonable expectation? We will examine the limits placed upon mass splittings of members of electroweak isodoublets by measurements of the ρ -parameter in Section IV and find that this result is consistent with those bounds. However, to be near this result requires that $m_t(M_X) \gtrsim 100$ GeV and thus there must be a large splitting already occurring in this generation at the grand unification mass scale. For example, a reasonable guess of $m_t \approx 15$ GeV at the G.U.T. mass scale $\approx 10^{15}$ GeV leads to only $m_t \approx 50$ GeV at the threshold for t-quark production. This result reflects only the characteristic upward renormalization of m_t by $SU(3) \times SU(2) \times U(1)$ but does not involve the fixed point. Also, there are other constraints to be considered before we can accept such a large m_t value. We return to these points in Section IV.

Perhaps it is more promising to consider a fourth heavy generation in which the effects of the fixed point are very likely to be felt. To this possibility we turn presently.

III. ADDITIONAL HEAVY QUARKS AND LEPTONS

In the preceding section we argued that the t-quark mass, if determined by the RG fixed point, would have a value of ≈ 240 GeV. To reach this mass scale the t-quark must already have an effective mass ≈ 200 GeV at M_x and thus this result might be unreasonably large. If, then, the number of quark flavors is ≤ 6 our discussion is irrelevant. However, the possibility exists that there may be additional flavor generations beyond the usual three and, if so, such quarks and leptons must be heavy. Hence, for extra generations it becomes extremely interesting to apply the RG fixed point model to obtain relatively insensitive mass predictions.

Of course, there are problems in allowing additional flavors beyond $n_f = 6$. In particular, the BEGN² one loop analysis of constraints on the successful m_b and m_s predictions limits $n_f \leq 8$. Furthermore, Nanopoulos and Ross⁵ find that the two loop corrections strengthen this constraint by $\approx 20\%$, whence $n_f \leq 6$. The latter result we believe is subject to the criticism that the authors ignore the effects of order $g_H^3 g_C^2$, etc., such as in Fig. (5) which involve the heavy quark Higgs-Yukawa couplings and which, for our purpose, are of order g_C^5 , i.e., $g_H \sim g_C$. Since g_H effects can enter with opposite sign to g_C effects we conclude that the Nanopoulos-Ross constraint is incomplete for sufficiently large g_H . Of course, the g_H effects in two loops could reinforce to strengthen the N-R constraint. It is of some

interest to carry out an evaluation of these corrections.¹⁴ Nonetheless, it is possible that we may tolerate $n_f \leq 8$ and we will presently restrict ourselves to this limit.

First we consider the case of two large Yukawa coupling constants of members of a single very heavy quark generation which we refer to as (T, B) and we now ignore the corrections of order g_t^2 and assume no Cabibbo mixing to other generations. For such a system we have:

$$\begin{aligned} 16\pi^2 \frac{dg_T}{dt} &= g_T \left(\frac{9}{2} g_T^2 + \frac{3}{2} g_B^2 - 8g_C^2 - \kappa_T \right) \\ 16\pi^2 \frac{dg_B}{dt} &= g_B \left(\frac{9}{2} g_B^2 + \frac{3}{2} g_T^2 - 8g_C^2 - \kappa_B \right) \end{aligned} \quad (3.1)$$

with

$$\begin{aligned} \kappa_T &= \frac{9}{4} g_2^2 + \frac{17}{12} g_1^2 \\ \kappa_B &= \frac{9}{4} g_2^2 + \frac{5}{12} g_1^2 \end{aligned} \quad (3.2)$$

It is not possible to solve eq. (3.1) analytically though we can easily discuss the fixed point behavior. Let us presently ignore κ_T and κ_B , the $SU(2) \times U(1)$ corrections, and following our discussion of the t-quark case, replace g_C^2 by a constant value of \bar{g}_C^2 .

Equations (3.1) possess three fixed points (in addition to the trivial $g_T = g_B = 0$ case) for $g_T \geq 0$ and $g_B \geq 0$:

$$\begin{aligned}
\text{(I)} \quad g_B = 0 & \quad ; \quad \left(\frac{9}{2} g_T^2 - 8\bar{g}_C^2\right) = 0 \quad \text{or} \quad g_T^2 = \frac{16}{9} \bar{g}_C^2 \\
\text{(II)} \quad g_T = 0 & \quad ; \quad \left(\frac{9}{2} g_B^2 - 8\bar{g}_C^2\right) = 0 \quad \text{or} \quad g_B^2 = \frac{16}{9} \bar{g}_C^2 \\
\text{(III)} \quad g_B = g_T = g \neq 0 & \quad ; \quad (6g^2 - 8\bar{g}_C^2) = 0 \quad \text{or} \quad g^2 = \frac{4}{3} \bar{g}_C^2 \quad . \quad (3.3)
\end{aligned}$$

We see that cases (I) and (II) are equivalent to the t-quark case. The more interesting fixed point is case (III).

We may examine the approach to the fixed points by considering small displacements and linearizing. For case (III) let $g_t = g + \delta g_t$, $g_b = g + \delta g_b$ and obtain:

$$\begin{aligned}
16\pi^2 \frac{d}{dt} \delta g_t &= 9g^2 \delta g_t + 3g^2 \delta g_b \\
16\pi^2 \frac{d}{dt} \delta g_b &= 9g^2 \delta g_b + 3g^2 \delta g_t \quad . \quad (3.4)
\end{aligned}$$

Using $g^2 = 4/3 \bar{g}_C^2$ and diagonalizing we find:

$$\begin{aligned}
16\pi^2 \frac{d}{dt} \delta g_1 &= 16\bar{g}_C^2 \delta g_1 \\
16\pi^2 \frac{d}{dt} \delta g_2 &= 8\bar{g}_C^2 \delta g_2 \quad (3.5)
\end{aligned}$$

with $\delta g_1 = \delta g_t + \delta g_b$, $\delta g_2 = \delta g_t - \delta g_b$. Hence, for decreasing t, the positivity of the eigenvalues implies that the fixed point is stable and $\delta g_i \rightarrow 0$ as $t \rightarrow 0$. (We've analyzed the general case of 2n quarks and prove that all fixed points for $g_i \geq 0$ are stable.)

If we return to the case of a running coupling constant, $g_c(t)$ we can still locate the fixed points exactly by exploiting the symmetry $g_T \leftrightarrow g_B$ of eq. (3.1). In case (III) consider

$$16\pi^2 \frac{dg}{dt} = g(6g^2 - 8g_c^2) \quad (3.6)$$

with solution:

$$g^2 = g_o^2 \left(\frac{g_c^2(t)}{g_c^2(t_o)} \right)^{8/b_o} \left\{ 1 + \frac{1}{6} \frac{g_o^2}{g_c^2(t_o)} \left\{ \left(\frac{g_c^2(t)}{g_c^2(t_o)} \right)^{1/b_o} - 1 \right\} \right\}^{-1} . \quad (3.7)$$

Repeating the discussion of Section (II) we are led to the intermediate fixed point behavior determined by an effective constant \bar{g}_c^2 :

$$\bar{g}_c^2 = \frac{b_o}{8} \frac{g_c(t)}{\ln R} \quad (3.8)$$

Apart from the choice of $n_f = 8$, this is the same effective constant determining the behavior in the t-quark case, which illustrates our discussion of the universality of the effective constant \bar{g}_c^2 in Section II.

We now turn to a numerical integration of eq. (3.1) in which we retain the effects of κ_T and κ_B , which slightly destroy the $g_T \leftrightarrow g_B$ symmetry through the small U(1) effects. We assume the coupling constants of Section II and presently extrapolate through an assumed heavy fermion threshold at $\mu \approx 200$ GeV (we assume a full SU(5) flavor generation here to maintain anomaly cancellation). The resulting extrapolated coupling constants become:

$$\begin{aligned}
\alpha_s &\approx \frac{1.108}{(t + 2.68)} \\
\alpha_2 &\approx \frac{3.142}{(t + 89.04)} & t = \ln \mu \\
\alpha_1 &\approx \frac{1.178}{(121.46 - t)} & (3.9)
\end{aligned}$$

which are okay to one-loop precision. In our present analysis, we do not worry about the self-consistent threshold condition of eq. (2.34) and carry our integration from $M_x \approx 10^{15}$ GeV down to $\mu \approx 200$ GeV.

Our results are presented in Fig. (6) as a scatter plot in which $g_T(M_x)$ and $g_B(M_x)$ are members of a 5×5 array taking on integer values (n, m) for $n \leq 4$, $m \leq 4$. These points are integrated down to $\mu \approx 200$ GeV and are found to cluster about the fixed points and a "domain wall" as shown in Fig. (6). In fact, the approach to the fixed points is more impressive than we show as the domain wall may be rigorously regarded as a mapping of array points at ∞ for $\mu = M_x$ to their intermediate fixed point values for $\mu \approx 200$ GeV. The density of clustering is sufficiently large that not all of the final $\mu \approx 200$ GeV array points are resolvable on our diagram. We have also indicated the initial direction of "flow" of the points at M_x .

Obviously, the fixed point of case (I) corresponds to the single heavy t-quark. From the present analysis we have:

$$\begin{aligned}
\text{case I: } & m_t \approx 255 & m_b = 0 \\
\text{case II: } & m_t = 0 & m_b \approx 250 \\
\text{case III: } & m_t \approx 222 & m_b \approx 217 & (3.10)
\end{aligned}$$

the discrepancy in case I is due to our lack of use of the threshold self-consistency condition of eq. (2.38) in eq. (3.10) and the new α_3 , which is now larger than before with $n_f = 8$ and increases the results.

It is not hard to estimate the curve that constitutes the domain wall in Fig. (6), though we have not performed a rigorous analysis of this curve. Hence, we can roughly patch it together by considering the two cases $g_T > g_B$ or $g_B > g_T$ (ignoring κ_T and κ_B effects presently which restores the symmetry $g_B \leftrightarrow g_T$). For example, for $g_T > g_B$ we must find a curve that interpolates between case (I) and case (III) of eq. (3.1). Hence, we have

$$\begin{aligned} g_T &= \left(\frac{16}{9} g_c^2 - \frac{1}{3} g_B^2 \right)^{1/2} & g_T > g_B \\ g_B &= \left(\frac{16}{9} g_c^2 - \frac{1}{3} g_T^2 \right)^{1/2} & g_B > g_T \end{aligned} \quad (3.11)$$

as crude approximations to the two patches of the domain wall. A more rigorous analysis of this kind of behavior would be interesting. We note that the numerical clustering about the entire domain wall suggests that this is a more general feature of our intermediate fixed point behavior. If a fourth generation pair of heavy quarks is discovered not satisfying the fixed point conditions of eq. (3.10) it is of interest to check if the masses are near to the domain wall conditions of eq. (3.11).

A more realistic possibility is that of a fourth SU(5) generation with a heavy lepton. Again, we make the simplifying assumption of ignoring Cabibbo mixing with lighter flavors and we also ignore any neutrino mass. Then, the three Higgs-Yukawa coupling constants g_T, g_B, g_E satisfy:

$$16\pi^2 \frac{d}{dt} g_T = g_T \left(\frac{9}{2} g_T^2 + \frac{3}{2} g_B^2 + g_E^2 - 8g_c^2 - \frac{9}{4} g^2 - \frac{17}{12} g'^2 \right)$$

$$\begin{aligned}
16\pi^2 \frac{d}{dt} g_B &= g_B \left(\frac{9}{2} g_B^2 + \frac{3}{2} g_T^2 + g_E^2 - 8g_C^2 - \frac{9}{4} g^2 - \frac{5}{12} g'^2 \right) \\
16\pi^2 \frac{d}{dt} g_E &= g_E \left(\frac{5}{2} g_E^2 + 3g_T^2 + 3g_B^2 - \frac{9}{4} g^2 - \frac{15}{4} g'^2 \right) .
\end{aligned} \tag{3.12}$$

It is clear from the above equations that the leptonic mass will be much smaller than the quark mass since it does not receive contributions from g_C^2 .

We will integrate eq. (3.12) numerically assuming the SU(5) relation at M_X , $g_B = g_E$. Without this assumption we would have a greater distribution of possible masses. With the SU(5) constraint we can present the result as a two-dimensional scatter plot as before for a 5×5 initial array of points (g_T, g_B) or (g_T, g_E) taking on integer values (m, n) at M_X .

In Fig. (7) we present the results of our numerical integration for (g_T, g_B) and (g_T, g_E) . This is qualitatively similar to the two quark case discussed previously. We observe three fixed points in analogy with the three cases discussed above:

$$\begin{aligned}
\text{case (I)} \quad g_B = g_E = 0 \quad g_T &\approx 1.45 \\
\text{case (II)} \quad g_T = 0 \quad g_B &\approx 1.36 \quad g_E \approx .628 \\
\text{case (III)} \quad g_T &\approx 1.25 \quad g_B \approx 1.23 \quad g_E \approx .342 .
\end{aligned} \tag{3.13}$$

Case (III) corresponds to masses $m_T \approx 219$, $m_B \approx 215$ and $m_E \approx 60$. Forthcoming accelerators may be able to observe such a lepton in the neighborhood of 60 GeV. If so, it would give significant encouragement to consider an effort to search for quark partners at the indicated energies.

These predictions would be different if one included a fifth heavy generation, or a heavy neutrino, or mixing angle effects. Our present discussion was aimed at getting a number characteristic of heavy lepton masses in the simplest set of assumptions. We have not yet carried out a study of the sensitivity of these results to various modifications as described above.

IV. FURTHER CONSIDERATIONS

In the present section we discuss various constraints appearing in the literature concerning fermion masses. Pendleton and Ross discuss several limits on the t-quark each of which become potentially more critical as our prediction increases the mass to ~ 240 GeV. The character of some of the limits changes slightly for our SU(5) heavy fourth generation, discussed in the preceding section. The constraints divide between "hard" experimental limits on radiative corrections to various processes and unitarity bounds and "soft" limits which appeal to the Higgs effective potential stability and perturbativity. We find that our predictions are consistent with all such bounds.

Veltman considers limits on fermion masses in the standard model from radiative corrections to neutral current cross sections.¹⁵ These emerge as essentially limits on the mass differences of members in a weak isodoublet, and we will naively apply them to quark doublets ignoring QCD corrections (presumably valid for sufficiently heavy quarks). In terms of the " ρ " parameter for a pair of massive fermions in a weak isodoublet with masses m_1 and m_2 we have:

$$\rho \equiv \frac{M_W^2}{M_Z^2 \cos^2 \theta_W} = 1 + \frac{G_F}{8\pi^2} \left\{ m_1^2 + m_2^2 - \frac{2m_1^2 m_2^2}{m_2^2 - m_1^2} \ln \frac{m_2^2}{m_1^2} \right\} \times \left\{ \begin{array}{l} 3 \text{ for quarks} \\ 1 \text{ for leptons} \end{array} \right\}. \quad (4.1)$$

Experimentally ρ is quite close to unity. Kim et al.¹⁶ in giving a phenomenological discussion of existing neutral current data quote a resulting world average of $\rho = 1.018 \pm .045$, or about a maximum tolerable 5% departure from unity. Improved constraints arise by making specialized assumptions, e.g. for internal consistency our model has assumed no right-handed isodoublets and we should use a ρ parameter of $1.002 \pm .015$, closer to a $\approx 2\%$ departure from unity at most. Applying these limits:

$$\frac{1}{m_p^2} \left\{ m_1^2 + m_2^2 - \frac{2m_1^2 m_2^2}{(m_2^2 - m_1^2)} \ln \frac{m_2^2}{m_1^2} \right\} \times \left\{ \begin{array}{l} 3 \text{ quarks} \\ 1 \text{ lepton} \end{array} \right\} \lesssim \left\{ \begin{array}{l} 5.5 \times 10^5 \text{ (5\%)} \\ 2.1 \times 10^5 \text{ (2\%)} \end{array} \right\} \quad (4.2)$$

hence, for a single heavy t-quark with $m_b \approx 0$ we have:

$$m_t \lesssim \left\{ \begin{array}{l} 420 \text{ GeV (5\%)} \\ 260 \text{ GeV (2\%)} \end{array} \right. \quad (4.3)$$

For our fourth heavy SU(5) generation near the nontrivial fixed point the above constraint applies to the difference $m_T - m_B$, ignoring the lepton contribution which is justified. Of course, improved accuracy in the determination of ρ may lead to improved limits on mass differences (with a required improvement in the analysis); however, our fourth generation heavy fermion prediction at the case (III) fixed point of Section III does not seem likely to violate this constraint. It is interesting that we might rule out case (I) and case (II) with slight improvements in ρ as well as ruling out the single fixed point t-quark.

Chanowitz et al.¹⁷ discuss other constraints on the fermion masses emerging from considerations of partial wave unitarity and perturbativity of heavy weak fermion scattering far above threshold. For N nearly degenerate isodoublets in the

standard model, quark masses must be less than $500/\sqrt{N}$ GeV while leptons must be less than $1 \text{ TeV}/\sqrt{N}$. These limits are easily satisfied by the upper bounds we obtain from the renormalization group evolution. All else being equal, for $N > 4$ we would begin to run afoul of this bound.

For completeness, we recall the Nanopoulos-Ross constraint on n_f from the successful SU(5) relations m_b/m_τ and m_s/m_τ .⁵ As we've mentioned earlier, these limits of $n_f \leq 6$ were obtained by ignoring contributions of order $g_H^3 g_{\text{QCD}}^2$ which for $g_H \sim g_{\text{QCD}}$, as in our work, may be important. If such contributions enter with the opposite sign then there will be a critical value g_{HC} such that for $g_H > g_{\text{HC}}$ we can have additional heavy fermions, provided of course that this lower bound is consistent with the aforementioned upper bounds. If, however, the sign of these effects reinforces the Nanopoulos-Ross contributions, then we cannot have $n_f > 6$ and, moreover, we would have an upper bound on g_t , e.g. $\leq g_{\text{HC}}$, hence an upper bound on m_t , emerging from two loops. This is clearly an interesting calculation¹⁴ and should produce "interesting" information either way and could be a sore point for $n_f > 6$, or else allow an interesting "window" for heavy quarks.

To one loop accuracy we must ask how the relationships m_b/m_τ and m_s/m_τ are affected by heavy fermions or a heavy t-quark. The effect upon m_b/m_τ has been discussed in ref. (3) in their case of $m_t \sim 135 \text{ GeV}$. Here we must include the effects of a mixing angle, θ , such that the charged weak current of t and b is $\cos \theta \bar{t} \gamma_\mu b_L$. The evolution of g_b/g_τ is given by (dropping terms of order $g^2, g_s^2, g_b^2, g_\tau^2$):

$$16\pi^2 \frac{d}{dt} \ln(g_b/g_\tau) = -\frac{3}{2} \cos^2 \theta g_t^2 - 8g_c^2 \quad . \quad (4.4)$$

Assuming g_t is at its fixed point value over most of the evolution from M_x , $g_t = \bar{g}_t$, which we take to a constant, we find upon integrating eq. (4.4):

$$\frac{g_b}{g_\tau} = \frac{m_b}{m_\tau} = \left(\frac{m_b}{m_\tau} \right)_{\text{(usual SU(5) prediction)}} \left(\frac{M_x}{m_t} \right)^{\frac{3\cos^2\theta - 2}{32\pi^2 \bar{g}_t}} \quad (4.5)$$

Any lighter (-1/3) quark mixing to the t-quark with $\sin \theta$ yields a correction factor:

$$\frac{m_D}{m_L} = \left(\frac{m_D}{m_L} \right)_{\text{(usual SU(5) prediction)}} \left(\frac{M_x}{m_t} \right)^{\frac{3\sin^2\theta - 2}{32\pi^2 \bar{g}_t}} \quad (4.6)$$

With a typical value of $\bar{g}_t^2 \approx 1.88$ and taking $\theta \approx 0$ we find the correction factor in eq. (4.5) to the m_b/m_τ value is a factor of $\approx (1.73)$. This is an upper bound and can be made closer to unity by choosing nonzero θ .

For the case of a heavy fourth generation and a light t-quark in SU(5) there are no renormalization effects upon m_b/m_τ and m_s/m_μ in the absence of mixing, whence we obtain results as in eq. (4.6). This arises because the contributions of heavy quarks and leptons to the light fermions is the same for light quarks and leptons. Hence, to one loop order, the successful SU(5) predictions are not significantly modified while the two-loop effects are not completely known.

One obtains "soft" bounds from consideration of the stability of the Higgs-effective potential in the presence of one-loop radiative corrections.^{18,19} For example, Hung¹⁹ discusses a stringent bound by demanding that the effective potential is bounded below as $\langle 0 | \phi | 0 \rangle = v$ tends to ∞ and simultaneously requiring that the quartic coupling constant λ be less than unity. For a single heavy t-quark

this amounts to $m_t \lesssim 134$ GeV, however there are several reasons to question the utility of this result. Similarly, Politzer and Wolfram¹⁹ argue $m_t \lesssim 300$ GeV with a certain assumption about perturbativity.

As mentioned by Hung himself, one may consider λ to be much larger than unity and still retain perturbativity. λ is bounded by $\sqrt{16\pi}$ by unitarity in which case the above quoted bound is significantly relaxed to $(\sum m_f^4)^{1/4} \lesssim 873$ GeV. This latter constraint is very insensitive to the number of fermions and, for an SU(5) generation with $m_T \approx m_B \approx m_E \approx m$, yields $m \lesssim 536$ GeV (including quark color factors) easily satisfied by our predictions and upper bounds.

Secondly, the unboundedness of the Higgs effective potential is only realized for v becoming so large that the calculation to one loop order is no longer self-consistent. For example, let us imagine that the quartic coupling constant of the Higgs potential is due entirely to the radiative corrections coming from a single heavy fermion with Higgs-Yukawa coupling g_H . From the formulae of Hung

$$V(\phi) = -\frac{1}{2}\mu^2\phi^2 + \frac{\lambda_{\text{int}}}{4!}\phi^4 + \kappa\phi^4 \ln \frac{\phi^2}{\langle\phi\rangle^2} \quad (4.7)$$

where

$$\kappa = \left\{ \frac{\lambda^2}{4} - 4g_H^2 \right\} \frac{1}{64\pi^2} \quad (4.8)$$

$$\lambda_{\text{int}} = \lambda - 100\kappa \quad (4.9)$$

and we determine $\langle\phi\rangle$ following Hung's renormalization conditions (eqs. (5, 6 and 7)):

$$\langle \phi \rangle^2 = \frac{\mu^2}{2\kappa + \frac{1}{6}\lambda_{\text{int}}} \quad . \quad (4.10)$$

If we consider $\lambda = 0$ we find:

$$\langle \phi \rangle^2 = \frac{3\mu^2}{176 g_H^2} \quad (4.11)$$

and

$$V(\phi) = -\frac{1}{2}\mu^2\phi^2 + \frac{1}{3!}\frac{g_H^2}{16\pi^2} \left\{ 100 - 4!! \ln \frac{\phi^2}{\langle \phi \rangle^2} \right\} \phi^4 \quad . \quad (4.12)$$

When does the potential become unbounded below? This requires that the second term of eq. (4.12) becomes negative, or

$$\phi^2 > \langle \phi \rangle^2 \exp\left(\frac{100}{4!}\right) = \frac{3\mu^2}{176 g_H^2} \exp\left(\frac{100}{4!}\right) \quad . \quad (4.13)$$

Regardless of the numerical result, eq. (4.3) indicates that perturbation theory is breaking down as the potential turns over, or upon substituting back into eq. (4.12) $V(\phi) \sim \mu^4/g_H^2$, a nonperturbative result. Presumably, including still higher order corrections will not remedy this situation. Hence, we do not believe that constraints of this kind are valid even in principle. This differs from ref. (18) in which one can conclude that the effective potential is unstable within the perturbative domain but that the minimum is located beyond the perturbative domain.

A final minor objection to Higgs-potential constraints is the fact that the gauge hierarchy problem of SU(5) is not understood and the interplay between that and our present considerations is unknown.

Beyond these considerations, which our model seems to survive, are the assumptions we've employed and the expectation of their validity. In our SU(5) analysis we've assumed zero mixing angle effects and our predictions are subject to corrections from mixing angles significantly larger than a few degrees. About this we can make few comments since the Kobayashi-Maskawa angles are known so poorly beyond θ_{Cabibbo} (most constraints are consistent with $\sin \theta_1 \approx 1/10$).²⁰ The fixed point value of m_t , if $n_f = 3$, is insensitive to mixing angle effects.

In all our discussion we've assumed a desert between M_W and M_Z to M_X , in which only the $SU(2) \times U(1) \times SU(3)$ interactions play a significant role and we've further assumed a point-like isodoublet Higgs boson over the full range of desert mass scales. Indeed, our starting point at eq. (2.3) is invalidated if the Higgs boson is not point-like above some mass scale M' in the desert. Since M' may well be a technicolor mass scale ~ 1 to 10 TeV, our results are evidently lost if the Higgs isodoublet is a composite technipion. Of course, so too are the SU(5) scenarios, such as m_b/m_τ . Hence, the RG fixed point model is intrinsically a GUT theory model with a standard GUT unification scale $\sim M_X$ and a standard desert extending up to that scale.

Finally, we comment that if GUT's are real, our results are at least very stringent bounds upon the masses of fermions assuming only perturbativity at M_X . This point has already been made by Cabibbo et al.²¹ Indeed, these bounds excel all of the others discussed in this section, provided GUT's are real.

It is compelling, therefore, that the quark mass scale ≈ 240 GeV seems to play a central role in the renormalization group equations of $SU(2) \times U(1) \times SU(3)$ in the GUT-desert picture. It might seem appropriate to consider seriously the related questions such as the phenomenology and experimental feasibility of

searches in this energy neighborhood in future machines, as well as improvements in the accuracy of the ρ -parameter and two-loop analysis including $g_H^3 g_{\text{QCD}}^2$ and g_H^5 effects in m_b/m_τ .¹⁴

ACKNOWLEDGMENTS

I wish to thank W.A. Bardeen, J.D. Bjorken, A.J. Buras, C. Quigg, M. Veltman and G.G. Ross for useful conversations and suggestions in the course of this work.

REFERENCES

- ¹ H. Georgi and S.L. Glashow, Phys. Rev. Lett. 32, 438 (1974); also, M.A. de Crombrugghe, Phys. Letters 80B, 365 (1979); H. Georgi and D.V. Nanopoulos, Nucl. Phys. B155, 52 (1979); H. Fritzsch, Nucl. Phys. B155, 189 (1979).
- ² A.J. Buras, J. Ellis, M.K. Gaillard and D.V. Nanopoulos, Nuclear Physics B135, 66 (1978).
- ³ B. Pendleton and G.G. Ross, Mass and Mixing Angle Predictions from Infrared Fixed Points, Oxford University Preprint, Oct. 1980.
- ⁴ See J. Ellis, 21st Scottish Universities Summer School, St. Andrews, Scotland, Ref. TH.2942/CERN; and our counterargument to ref. (5) in Sections (III, IV).
- ⁵ D.V. Nanopoulos and D.A. Ross, Nucl. Phys. B157, 273 (1979).
- ⁶ L. Maiani, G. Parisi and R. Petronzio, Nucl. Phys. B136, 115 (1978).
- ⁷ C.D. Froggatt and H.B. Nielsen, Nucl. Phys. B147, 277 (1979).
- ⁸ M. Veltman, The Infrared-Ultraviolet Connection, Ann Arbor Mich. Preprint, 1980, and private communications.
- ⁹ B. Pendleton and G.G. Ross, in preparation (private communication).
- ¹⁰ J. Sakurai in Proceedings of the Eighth Hawaiian Topical Conference in Particle Physics, Honolulu, 1979.
- ¹¹ T.P. Cheng, E. Eichten and L.F. Li, Phys. Rev. D9, 2259 (1974) or see ref. (3) and ref. (6).
- ¹² Our present discussion parallels that of J. Ellis, M.K. Gaillard, D.V. Nanopoulos and S. Rudaz, LAPP Preprint TH-24/Cern TH.2833 (1980).
- ¹³ H. Georgi and H.D. Politzer, Phys. Rev. D14, 1829 (1976).

- ¹⁴C.T. Hill, work in progress.
- ¹⁵M. Veltman, Nucl. Phys. B123, 89 (1979).
- ¹⁶J.E. Kim, P. Langacker, M. Levine, H.H. Williams, Univ. of Pennsylvania Preprint UPR-158T (1980).
- ¹⁷M.S. Chanowitz, M.A. Furman and I. Hinchliffe, Nucl. Phys. B153, 402 (1979).
- ¹⁸S. Coleman and E. Weinberg, Phys. Rev. D7, 1888 (1973).
- ¹⁹P.Q. Hung, Phys. Rev. Letters 42, 873 (1979); see also H.D. Politzer and S. Wolfram, Phys. Lett. 82B, 242 (1979) and Errata 83B, 421 (1979).
- ²⁰L. Wolfenstein, Nucl. Phys. B150, 501 (1979).
- ²¹N. Cabibbo, L. Maiani, G. Parisi and R. Petronzio, Nucl. Phys. B158, 295 (1979).
- ²²Since the completion of this paper Buras has obtained the stringent bound of $m_t \lesssim 40$ GeV from consideration of $K_L \rightarrow \mu^+ \mu^-$: A. Buras, Fermilab-Pub-81/27-THY. This result may be modified by the presence of a fourth generation.

FIGURE CAPTIONS

- Fig. 1: $g_t(100 \text{ GeV})$ against $g_t(M_X)$ including only effects of QCD indicating Pendleton-Ross fixed point and result assuming slowly varying g_{QCD}^2 using average, \bar{g}_c^2 , between $t = \ln(M_X)$ and $t = \ln(100)$.
- Fig. 2: Diagrams contributing to RG equations; $G \subset SU(3)$, $A \subset SU(2)$, $B \subset U(1)$, and dashed line is Higgs boson. Figs. (2b) and (2c) are also extrapolation contributions.
- Fig. 3: $g_t(\mu)$ against $g_t(M_X)$ for $\mu = 100 \text{ GeV}$, 10 GeV and 1 GeV . Arrow denotes location of PR fixed point and (+) denotes location of approximate intermediate fixed point using for \bar{g}_{QCD}^2 the average as in eq. (2.17).
- Fig. 4: Evolution of $g_t(\mu)$ for several initial choices of $g_0 \equiv g_t(M_W)$. We plot also the PR fixed point condition of eq. (2.13) and the intermediate fixed point of eq. (2.22). Also, we include the self-consistent threshold condition of eq. (2.23).
- Fig. 5: Sample higher order corrections to the analysis of ref. (5) important when $g_H \sim g_{\text{QCD}}$.
- Fig. 6: Scatter plot result of numerical integration of eq. (3.1) with 5×5 initial array.
- Fig. 7: Scatter plots resulting from numerical integration of eq. (3.12) relevant to an $SU(5)$ fourth generation with 5×5 initial array as in Fig. 6.

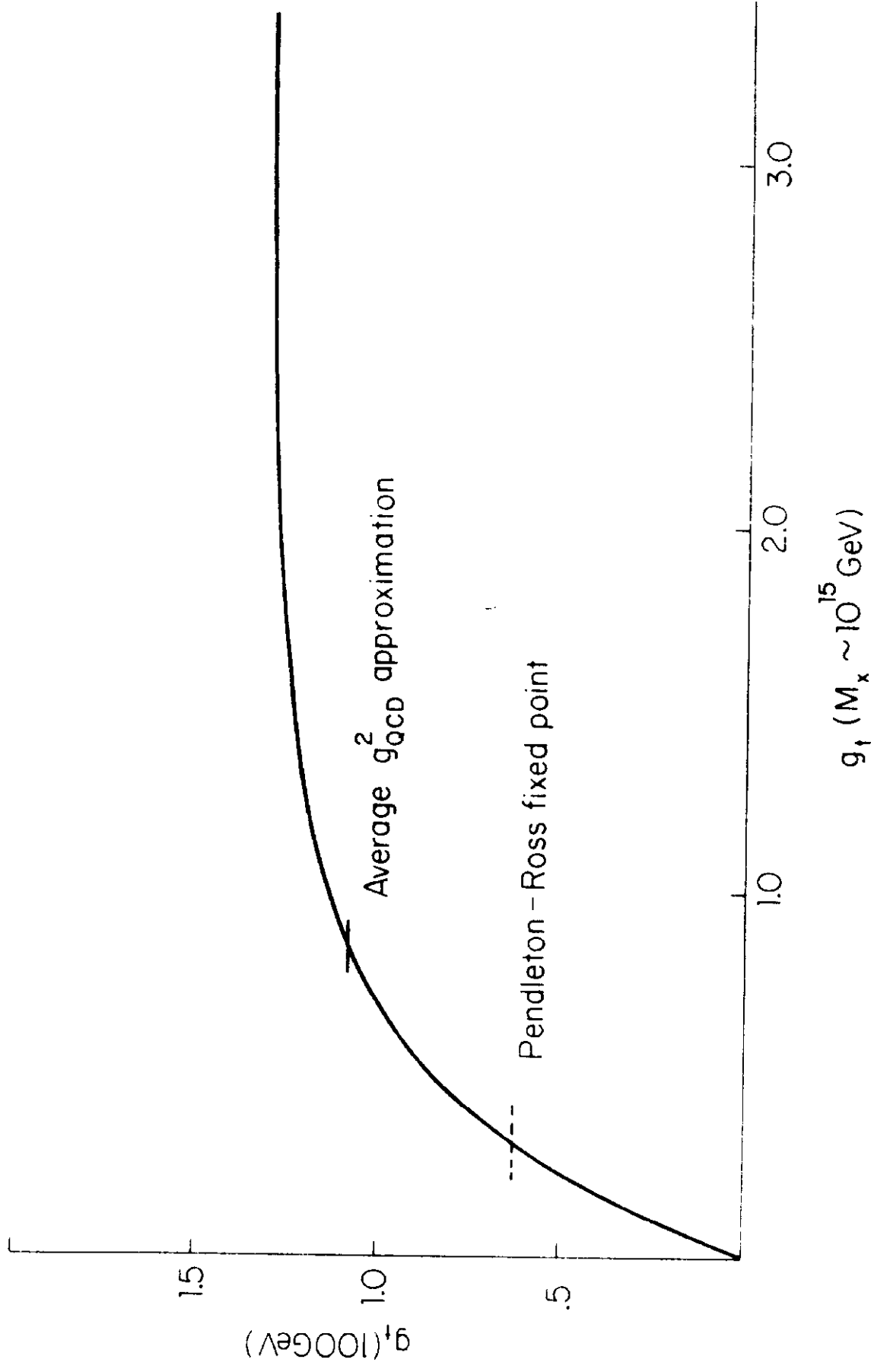
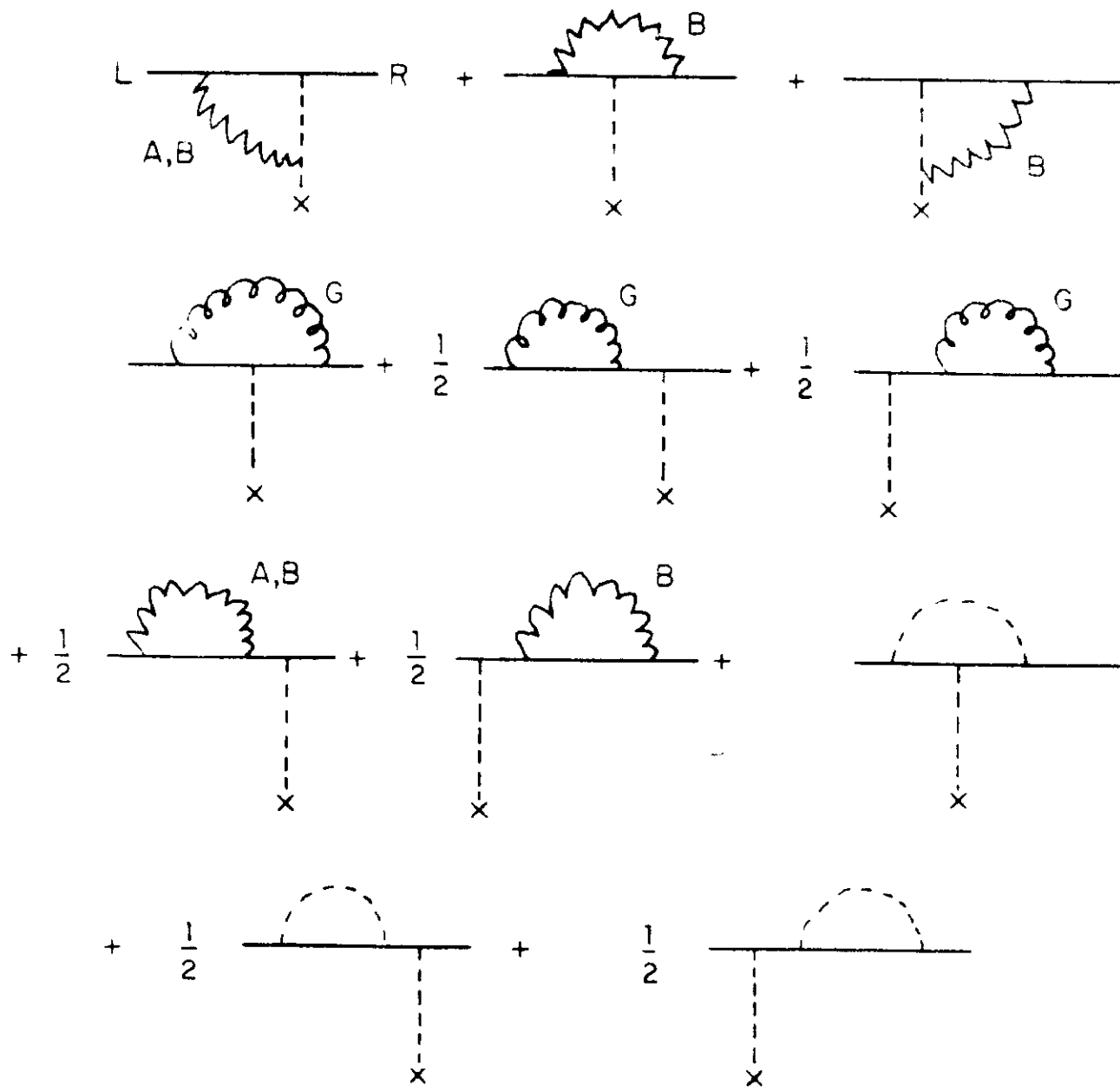
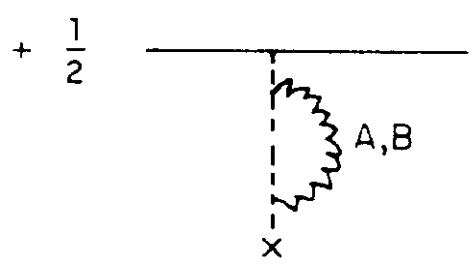


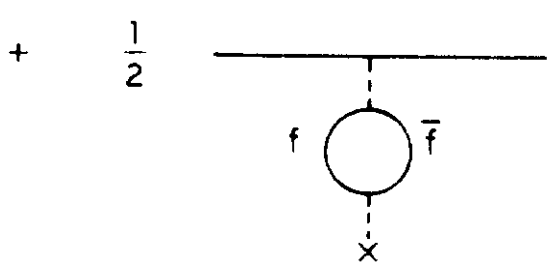
Fig. 1



(2a)



(2b)



(2c)

Fig. 2

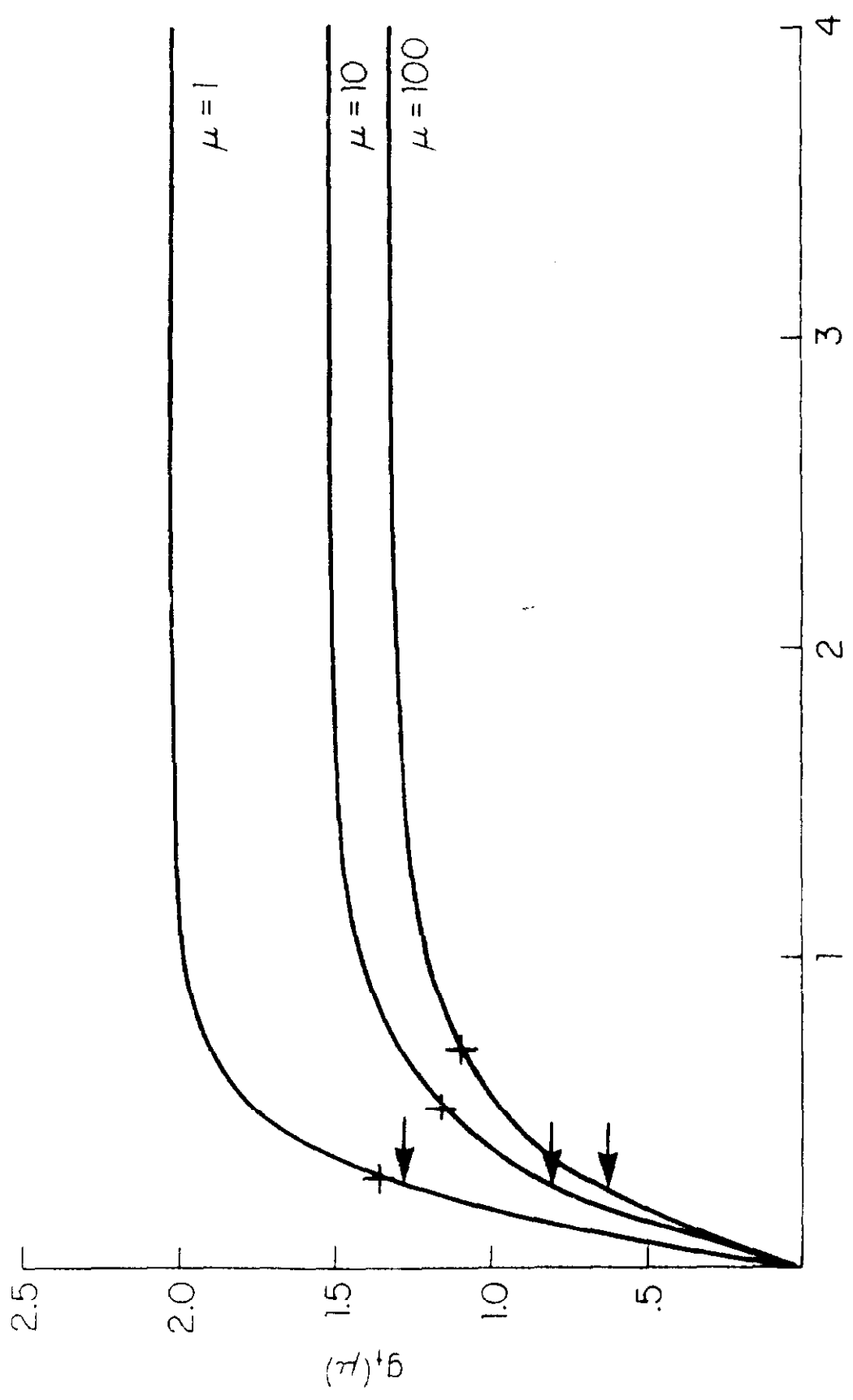
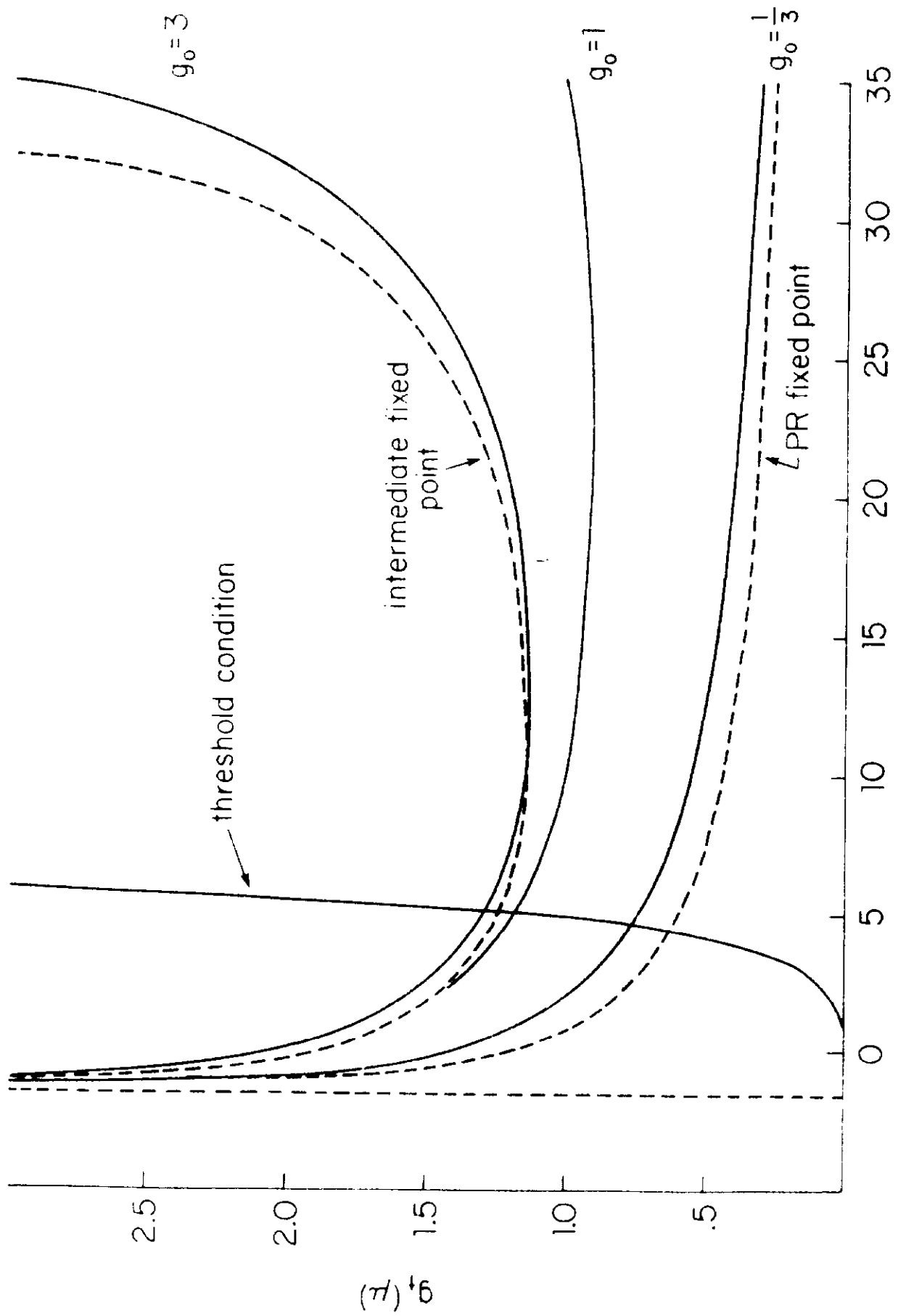


Fig. 3



$\ln \mu$

Fig. 4

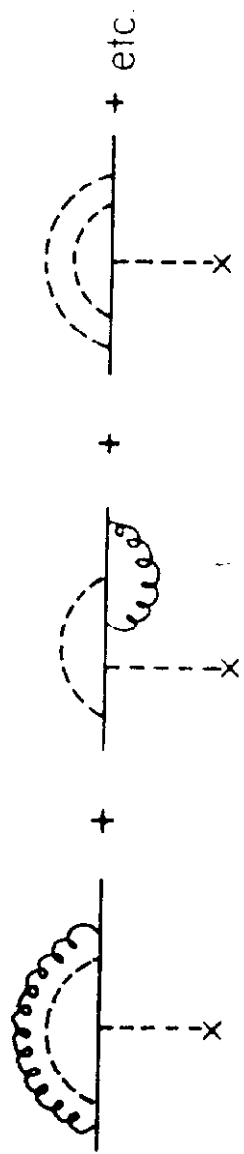


Fig. 5

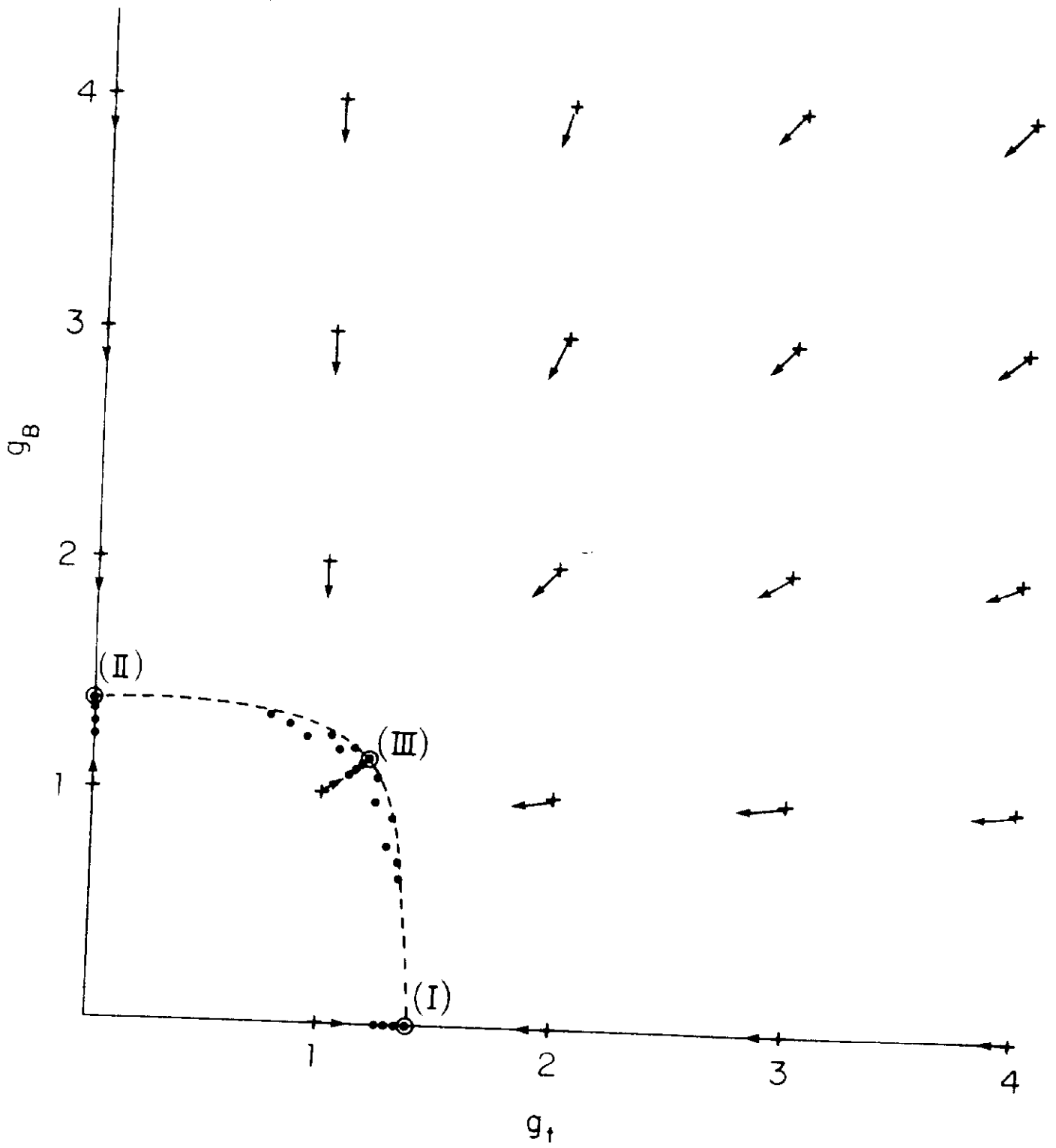


Fig. 6

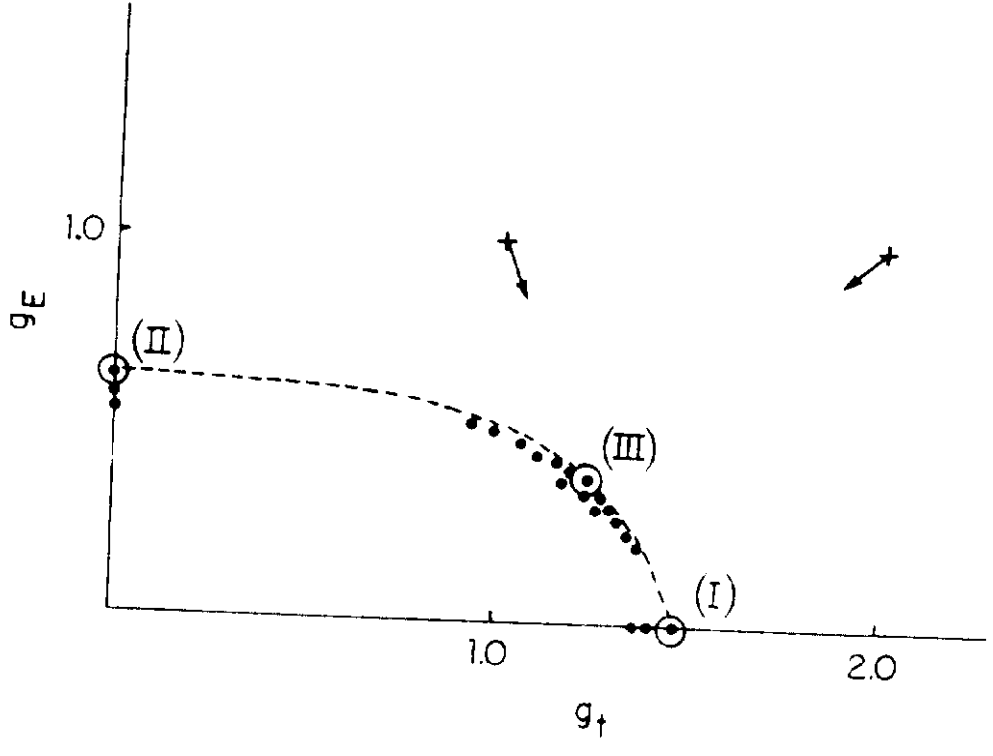
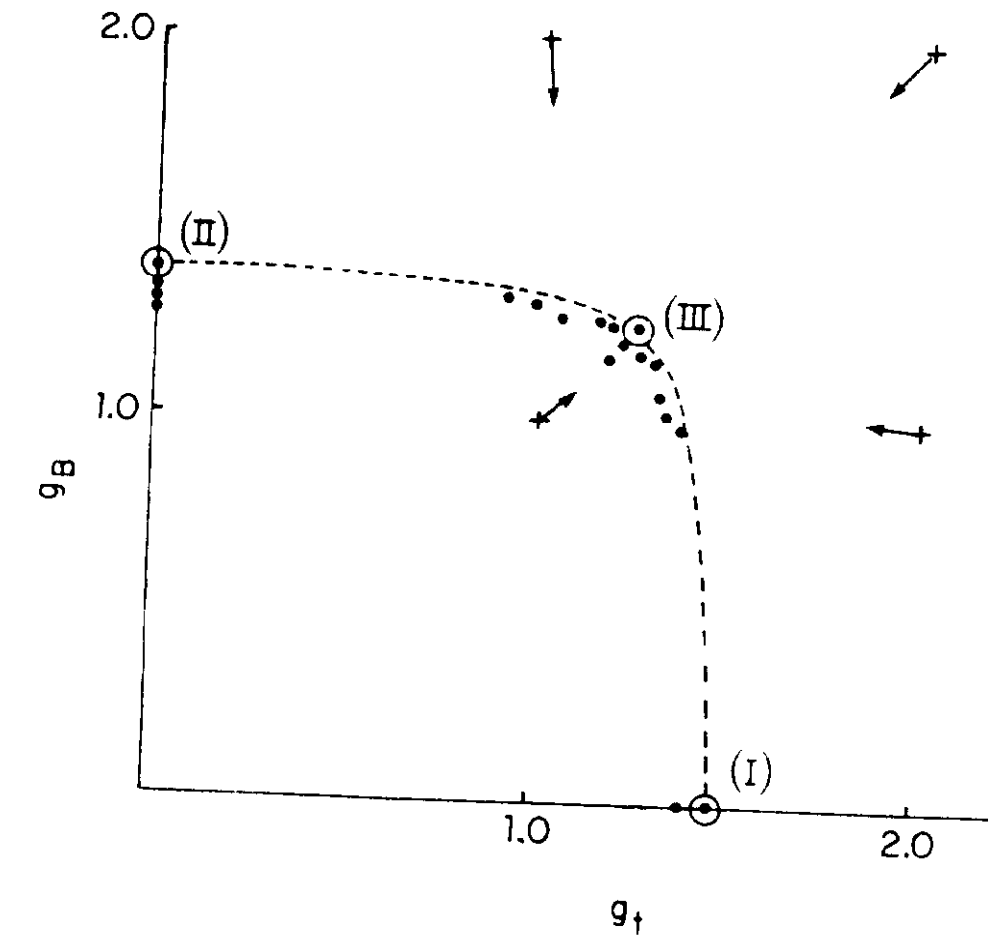


Fig. 7